ResearchGate

See discussions, stats, and author profiles for this publication at: https://www.researchgate.net/publication/248816685

Arc dynamics and tectonic history of Fiji based on stress and kinematic analysis of dikes and faults of the Tavua Volcano, Viti Levu Island, Fiji

Article *in* Tectonics · August 2002

DOI: 10.1029/2000TC001259

CITATIONS
13

READS
84

2 authors, including:

Graham Begg
Macquarie University
39 PUBLICATIONS **1,651** CITATIONS

SEE PROFILE

Some of the authors of this publication are also working on these related projects:

Project Lithospheric Architecture Mapping of Phanerozoic orogens View project

Project Proterozoic assembly of southwestern Laurentia View project

All content following this page was uploaded by Graham Begg on 22 August 2017.

The user has requested enhancement of the downloaded file.

Arc dynamics and tectonic history of Fiji based on stress and kinematic analysis of dikes and faults of the Tavua Volcano, Viti Levu Island, Fiji

Graham Begg[1] and David R. Gray[2]

Victorian Institute of Earth and Planetary Sciences (VIEPS) School of Geosciences, Monash University, Melbourne, VIC, Australia

Received 28 August 2000; revised 16 October 2001; accepted 13 December 2001; published 13 July 2002.

[1] Stress analysis of dikes and kinematic analysis of faults within the Tavua Volcano of Viti Levu, Fiji, indicate an apparent migration of the causative maximum principal stress axis (σ_1) from NW toward north between ~5.0 and <3.9 Ma. The dikes and faults are part of successive structural and magmatic events at the arc scale. We present data on the chronological succession of stress indicators in the Tavua Volcano, based on overprinting relationships and published geochronology, which also equate with a counterclockwise rotation of Fiji, assuming an approximately constant N-S regional compressive stress orientation during this time. The latter interpretation is consistent with paleomagnetism studies that require substantial counterclockwise rotation of the Fiji Platform, since fragmentation of the formerly continuous Outer Melanesian Arc during the latest Miocene to earliest Pliocene. The stress data suggest that the Fiji platform has undergone an ~50° rotation since ~5 Ma. Given that rotation apparently stopped at 3 Ma, then particularly fast rotation of ~25° Myr^{-1} occurred from ~5 Ma to 3 Ma. Recent seismicity data indicate the platform is currently subject to N-S compression. The history of late Miocene and Pliocene events in the region can be related to the consequences arising from collision of an island arc with an oceanic plateau. *INDEX TERMS:* 8010 Structural Geology: Fractures and faults; 8155 Tectonophysics: Plate motions—general; 9355 Information Related to Geographic Region: Pacific Ocean; *KEYWORDS:* stress, dikes, faults, kinematics, Fiji, tectonics

1. Introduction

[2] In oceanic plate settings, features such as dikes, sills, and faults in both ocean floor and volcanic arc sequences can be used as kinematic and dynamic (stress) indicators to track both changes in regional stress orientations and directions of plate motion [e.g., *Goscombe and Everard*, 2001]. Since *Anderson* [1936, 1951] postulated that volcanic dikes and sills intrude parallel to the local $\sigma_1-\sigma_2$ plane with opening of their walls parallel to σ_3, dike trends have been used as dynamic indicators to map out regional stress trajectories and to determine principal stress directions [e.g., *Ode*, 1957; *Nakamura et al.*, 1977, 1980; *Muller and Pollard*, 1977]. The orientation and slip sense of contemporaneous strike-slip faults in active arc environments may also be used to resolve the principal horizontal stress directions responsible for their movement [e.g., *Arthaud*, 1969], and to establish the regional stress field of the associated tectonic setting.

[3] An abundance of dynamic and kinematic indicators at all observational scales over the Tavua Volcano, Fiji, and a well-defined chronology of events [*Setterfield et al.*, 1992; *Eaton and Setterfield*, 1993; *Begg*, 1996], allows a detailed examination of the stress history of the volcano and the island of Viti Levu, relative to the changing plate boundaries and plate configurations. Dikes and sills of different composition commonly reflect the evolving magma chamber through time and thereby provide a chronology of stress indicators that can therefore be used to track the regional stress field. In the Tavua Volcano these include precaldera absarokite (basalt) dikes and syncaldera shoshonite and banakite dikes, which, combined with stress orientation data from both caldera collapse and postcollapse fault structures, map out the rotation of Fiji over at least 1.3 m.y. during the Pliocene.

[4] Fiji provides a unique laboratory to investigate structures that have resulted from the stranding of an arc from the subduction process, with later uplift, rotation, and deformation as a result of back arc extension and shear deformation. The objectives of this paper are firstly, to document dike orientation and fault slip data from the Tavua Volcano, secondly, to place these data in a regional arc-scale context, and thirdly, to use them to investigate the stress history and rotation of Fiji over time. Stress orientation data show that the maximum compressive stress direction (σ_1) derived from stress indicators within the Tavua Caldera has changed through time because of events at the arc scale. These data support independent paleomagnetic evidence for counterclockwise rotation of Fiji between 10 Ma and 3 Ma.

2. Tectonic Setting of Fiji

[5] The Fiji Islands are situated on a prominent offset of the convergent boundary between the Pacific and Australian

[1]Now at Western Mining Corporation Limited (WMC) Resources, Belmont, WA, Australia.

[2]Now at School of Earth Sciences, The University of Melbourne, Melbourne, VIC, Australia.

Copyright 2002 by the American Geophysical Union.
0278-7407/02/2000TC001259$12.00

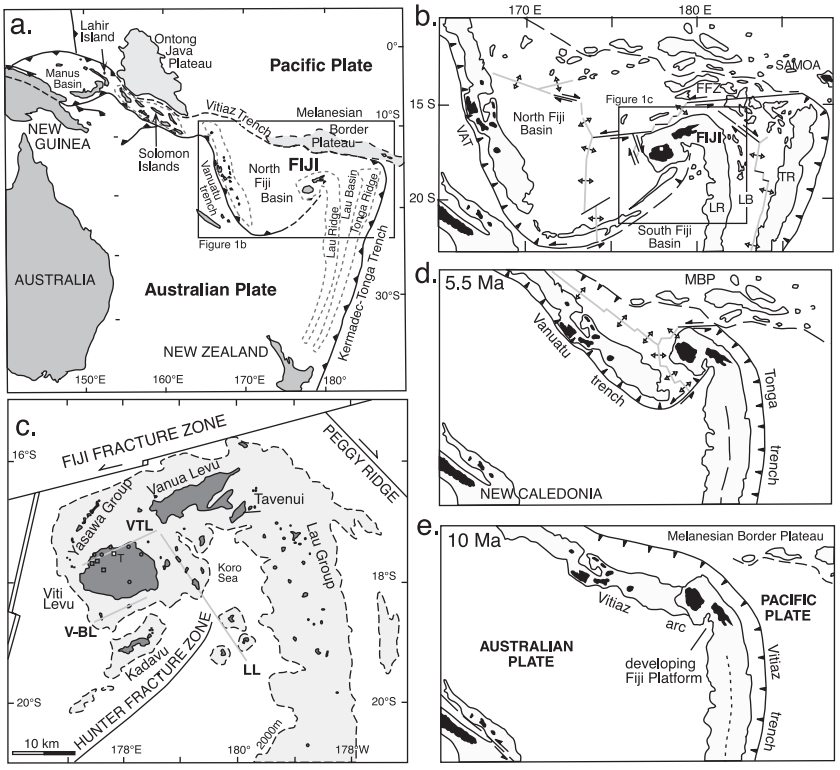

Figure 1. Tectonic setting (Figures 1a–1c) and tectonic reconstructions (Figures 1d and 1e) of the Outer Melanesian region (adapted from *Hathway* [1993]; reprinted with permission from the Geological Society of London). (a) Map of the Fiji platform and north end of the Lau Ridge showing the major islands in the Fiji area, the major early Pliocene volcanoes of Viti Levu, the major seafloor fracture zones, and part of the spreading center of the Fiji Basin (adapted from *Gill and Whelan* [1989]). Shoshonitic volcanoes, including the Tavua Volcano (T), are shown by squares and calc-alkaline volcanoes by circles. (b) Tectonic features of the northeastern segment of the plate boundary between the Australian and Pacific plates showing the Outer Melanesian Arc of the southwest Pacific, trenches and ridge systems, and oceanic plateaus (adapted from *Kroenke* [1984]). Fiji, as part of the Fiji Platform, consists of a series of islands at the north end of the Lau Ridge, with the North Fiji Basin formed as part of a spreading center. (c) Present plate configuration. (d) Reconstruction at 5.5 Ma. (e) Reconstruction at 10 Ma. In Figures 1a–1e the Australian plate is fixed and the east-west convergence rate between plates was assumed to be 9–10 cm yr^{-1}. Shading represents submarine depths <2000 m. Abbreviations are as follows: VT, Vitiaz trench; VAT, Vanuatu trench; LR, Lau Ridge; LB, Lau Basin; TR, Tonga Ridge; FFZ, Fiji Fracture Zone; LL, Lomaiviti lineament; V-BL, Vatulele-Beqa lineament. Long dashes denote southern margin of the Melanesian Border Plateau (MBP). The open square (Figures 1b and 1c) denotes the location of the Tavua Volcano.

tectonic plates (Figure 1). This offset marks a broad zone of diffuse spreading and transform faulting [*Hamburger and Isacks*, 1988] accommodating divergence of the east facing Tonga arc-trench system and the west facing Vanuatu arc-trench system by left lateral wrenching and opening of the North Fiji Basin. Active subduction is along the present-day Vanuatu and Tonga-Kermadec trenches. The low level of earthquake activity south of Viti Levu and the dominant strike-slip fault plane solutions indicate that subduction along the Hunter Fracture Zone (Figure 1c) has possibly ceased [*Hamburger and Everingham*, 1986]. This means that the Fiji Platform is again part of the Australian plate [*Rodda*, 1993]. The boundary between the Pacific and Australian plates is regarded to be the seismically active Fiji Fracture Zone [*Hamburger and Everingham*, 1986]. Recent paleomagnetic data suggest that rotation of the Fiji platform stopped abruptly at 3 Ma with the development of a well-defined spreading center in the North Fiji Basin [*Taylor et al.*, 2000].

[6] Current seismicity data show that while NE-SW shortening dominates in the vicinity of the left lateral Fiji Fracture Zone, it is progressively overshadowed by N-S shortening farther south on the Fiji Platform [*Hamburger and Isacks*, 1988]. The component of NE-ENE shortening may reflect transfer of stresses associated with sinistral slip of the Fiji Fracture Zone. In the Lau Basin and eastern North Fiji Basin current stress fields indicate N-S shortening and E-W extension along NW and NE striking strike-slip faults [*Hamburger et al.*, 1988]. Pliocene shoshonitic and calc-alkaline volcanic centers dominantly occur along three

lineaments in the Fiji region. Seven shoshonitic and high K calc-alkaline volcanic centers define the ENE trending Viti Levu lineament [*Rodda*, 1993]. The largest of these is the shoshonitic Tavua Volcano on the island of Viti Levu ("T" in Figure 1c). This lineament extends from northwest Viti Levu through Vanua Levu and coincides with the NE alignment of volcanic centers on the island of Tavueni. Two other lineaments, the NNW trending Lomaiviti lineament immediately east of Viti Levu and the ENE trending Vatulele-Beqa lineament immediately south of Viti Levu [*Gill and Whelan*, 1989; *Rodda*, 1993], are represented by island chains on margins of the Fiji Platform and are dominated by Pliocene shoshonitic plus lesser calc-alkaline volcanism.

[7] Further south of Viti Levu, just off the southern margin of the Fiji Platform, the Kadavu Islands lie immediately north of the Hunter Fracture Zone and trend between NE and ENE. They are composed of basaltic to dacitic shoshonitic to high-K and medium-K calc-alkaline volcanics ranging in age from 3.2 Ma to <1 Ma [*Rodda*, 1993]. There is one small volcano of alkali-basalt. To the west of Viti Levu, the Yasawa group of islands are dominated by late Miocene basaltic and andestic volcanism. Post-Miocene folding about axes parallel to the NNE to NE strike of the island chain is accompanied by southeast over northwest thrusting [*Rodda*, 1993]. East of Viti Levu, the islands of the Koro Sea consist of basaltic volcanoes with diverse geochemistry, including tholeiitic, calc-alkaline, shoshonitic, and alkaline [*Rodda*, 1993].

3. Tectonic History

[8] The magmatic, sedimentological, and structural processes that formed the Fiji Platform can be viewed as part of three distinct tectonic and volcanic phases of the Outer Melanesian Arc [see *Gill et al.*, 1984]: (1) Vitiaz arc phase (35–8 Ma); (2) transitional phase (8–3 Ma); and (3) present phase (3–0 Ma). The Vanuatu, Fiji, and Tonga Islands were once part of the continuous Vitiaz arc (Figure 1e), related to a west dipping subduction zone composed of the Tonga trench and extending northwest along the now relict Vitiaz trench to the eastern margin of the Solomon Islands arc [*Chase*, 1971; *Recy and Dupont*, 1982; *Colley and Hindle*, 1984; *Gill and Whelan*, 1989]. This arc system was active from the early Eocene to the middle Miocene [*Gill and McDougall*, 1973], until collision with the Melanesian Border Plateau, immediately north of Fiji [*Falvey*, 1975; *Gill and Whelan*, 1989], and the Ontong Java Plateau, farther north adjacent to the Solomon Islands [*Falvey*, 1975; L. W. Kroenke, Geology of the Ontong-Java Plateau, unpublished report 72-5, Hawaii Institute of Geophysics, 1972]. The timing of these collisions is not known precisely, but Ontong Java Plateau collision is thought to have occurred at about ~10 Ma [*Kroenke*, 1984, also unpublished report, 1972]. The Melanesian Border Plateau may, however, have collided with the arc east of Fiji as late as 7.5 Ma [*Gill and Whelan*, 1989; *Hathway*, 1993]. In Fiji, uplift, intrusion of trondjhemite ± gabbro, and accompanying low-temperature metamorphism occurred at ~10 Ma [*Rodda*, 1967], while further uplift associated with deformation seems to have occurred at ~7.5 Ma [*Hathway*, 1993]. The collisions effectively terminated subduction along the Vitiaz trench and led to reversal of arc polarity northwest of Fiji along the Vanuatu segment of the arc possibly as early as 8 Ma [*Hamburger and Isacks*, 1988; *Gill and Whelan*, 1989].

[9] At this time a new trench was established west of the Vanuatu arc (Figure 1e) [*Gill and Whelan*, 1989], where volcanism began to reflect the presence of the new subduction zone during the Pliocene [*Gill and Gorton*, 1973]. Between 8.0 and 5.5 Ma, fragmentation of the arc immediately north of Fiji formed a transverse rift, which became a transfer zone as back arc spreading allowed the opposite facing Vanuatu and Tonga arcs to diverge [*Whelan et al.*, 1985; *Gill et al.*, 1984]. Back arc spreading occurred initially in the North Fiji Basin and later in the Lau Basin. The spreading resulted in isolation of the inactive Vitiaz trench and the Lau Ridge (Figure 1b). Palaeomagnetic data indicate that the oldest rocks of the North Fiji Basin may be up to 8 Ma [*Malahoff et al.*, 1982], whereas the opening of the Lau Basin is thought to have occurred between 6 and 3 Ma [*Parson et al.*, 1990; *Taylor et al.*, 2000], but probably closer to 3 Ma [*Gill and Whelan*, 1989]. Shoshonitic volcanism, normally associated with arc extension-related volcanism [*Morrison*, 1980], occurred in Fiji as early as 5.5 Ma [*Gill and Whelan*, 1989].

[10] The northern part of the Lau Ridge adjacent to the transverse rift, incorporating the Fiji Islands, underwent counterclockwise rotation sometime after 5.5 Ma [*Whelan et al.*, 1985] and is now known as the Fiji Platform (broadly defined by the 2000 m bathymetric contour). Studies of paleomagnetic data on Viti Levu indicate 21°–60° of rotation during the past 3–5 m.y. [*Whelan et al.*, 1985; *Taylor et al.*, 2000], though *Malahoff et al.* [1982] claim up to 90° of rotation. New data from *Taylor et al.* [2000] suggest that the total counterclockwise rotation of the Fiji Platform from 10 Ma to 3 Ma is 135° (±17°), with the original arc facing east (compatible with *Musgrave and Firth* [1999]). They suggest that some 60°–65° of this rotation occurred before 6 Ma. Similarly, paleomagnetic data suggest that the Vanuatu island arc rotated 30° in a clockwise direction during the past 6 m.y. [*Falvey*, 1978], or 39° since the late Miocene [*Musgrave and Firth*, 1999]. Incipient northward subduction of the South Fiji Basin crust occurred along the southern margin of the Fiji Platform, defining the Hunter Fracture Zone (Hunter Fracture Zone (HFZ); Figures 1b and 1c). Along with the Fiji Fracture Zone (FFZ; Figures 1b and 1c) defining the northern margin of the Fiji Platform, the two fracture zones now define the southern and northern limits, respectively, of a diffuse E-W left lateral transfer zone linking the divergent Vanuatu and Tonga trenches (Figure 1c) [*Hamburger and Isacks*, 1988].

4. Stress and Kinematic Indicators and the Tavua Volcano

[11] The Tavua Volcano is the largest of seven shoshonitic to high-K calc-alkaline Pliocene volcanoes defining the ENE trending Viti Levu lineament on the island of Viti

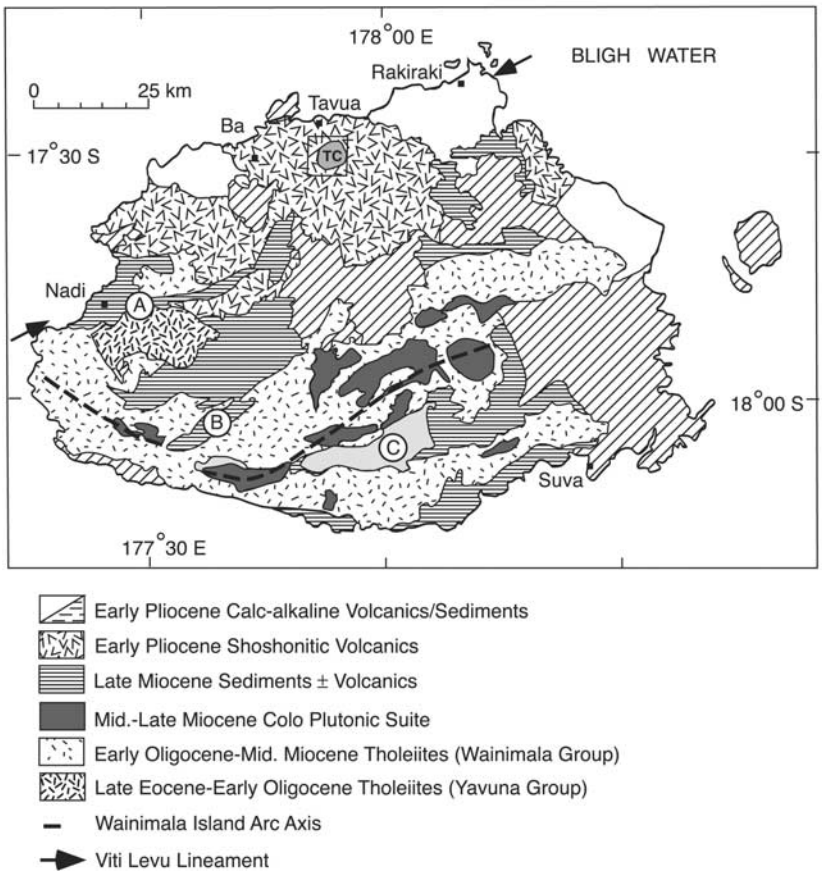

Figure 2. Geological map of the island of Viti Levu (adapted from *Rodda* [1984]). Remnants of the Vitiaz arc (Figure 1e) are the tholeiitic basalts of the late Eocene to early Oligocene Yavuna Group on the west side of the island. These are unconformably overlain by rocks of the Wainimala arc (Wainimala Group) of *Hathway* [1993] intruded by the Colo Plutonic Suite ranging from 12.5 to ~8 or 7 Ma [*Rodda and Kroenke*, 1984; *Whelan et al.*, 1985; *Rodda*, 1993; *Hathway*, 1994], that crop out as part of a ENE trending anticlinorium stretching across southern Viti Levu. The northern part of the island is dominated by early Pliocene shoshonitic volcanics, including the Tavua Volcano (TC, Tavua Caldera). The bold dashed line shows the position of the Wainimala Island arc axis and the bold arrows denote the position of the Viti Levu Lineament. Basins are labeled as follows: A, Nadi Basin; B, Sovi Basin; C, Navua Basin.

Levu, Fiji (Figure 2). The intrusive sequence of the volcano spans a period between 5.2 Ma and 4.4 Ma [*Whelan et al.*, 1985; *Setterfield et al.*, 1992]. Within the volcano, nested calderas filled with shoshonitic lavas (augite andesite, Turtle Pool Formation of the first caldera) and banakitic lavas (biotite andesite, Morrisons Pool Formation of the second caldera) (Figure 3) indicate two major sequential collapse episodes, respectively, associated with a total subsidence of ~3 km [*Setterfield et al.*, 1991; *Begg*, 1996]. Dikes associated with each caldera stage intrude older rocks across the volcano. Collapse resulted in extensive block faulting, development of a large number of steep faults, and tilting around the caldera margin, best exposed along the southwest margin in the workings of the Emperor gold mine (Figure 3). The Emperor low sulphidation epithermal gold deposit formed after cessation of volcanic activity [*Anderson and Eaton*, 1990; *Setterfield et al.*, 1992]. A summary of the relative timing of structural, magmatic, and hydrothermal events affecting the Tavua Volcano is presented in Figure 4.

4.1. Dikes

[12] Abundant dikes of compositions equivalent to all extrusive lava types of the Tavua Volcano occur within the precaldera stratigraphy, but lesser numbers of dikes occur within the caldera (Figure 3). Absarokite dikes do not occur within the Tavua Caldera, and shoshonite dikes do not occur within the Inner Caldera. Monzonite dikes are observed at depth within the Emperor gold mine. Crosscutting relationships consistently indicate that absarokite dikes are the oldest and banakite dikes are the youngest.

[13] Most dikes strike obliquely to the caldera margins, and ring dikes are rare. Precaldera absarokite dikes show WNW to NW trends, with lesser NNE-NE trends (Figure 5a).

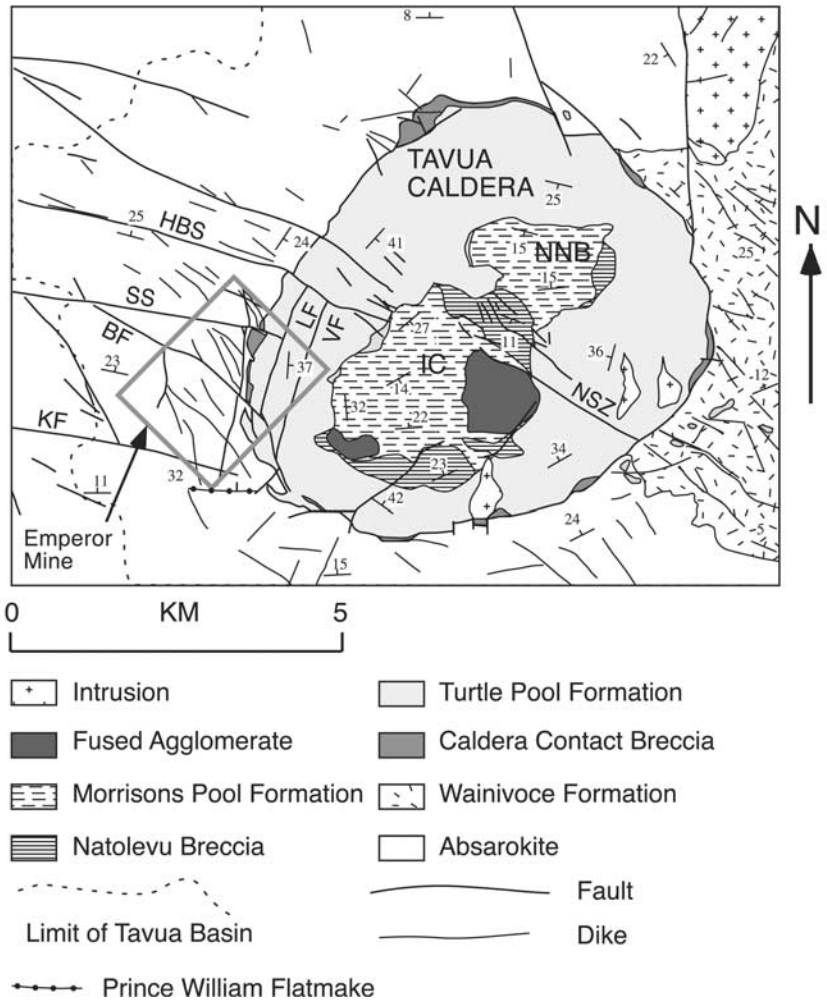

Figure 3. Simplified geology of the Tavua Basin. Adapted from mapping by Western Mining Corporation (Fiji) Ltd (WMC). Boundary between the precaldera (absarokite and Wainivoce Formation) and earliest syncaldera (caldera contact breccia and Turtle Pool Formation) material is known as the caldera contact. Abbreviations are as follows: IC, inner caldera; NNB, Natolevu North Basin; NSZ, Nasivi Shear Zone; HBS, Homeward Bound Shear; SS, Shatter Shear; BF, Brewster fault; KF, Koromakawa fault; LF, Lololevu fault; VF, Vunisina fault.

Though the total data mean is 311°, the individual sector means all lie between 270° and 305°, with the exception of the S sector (354°). The occurrence of north trends in the S sector and west trends in the E sector may reflect radial geometries with respect to the center of the volcano (now occupied by the caldera). Shoshonite (augite andesite) dikes contemporaneous with the infill of the initial caldera by the Turtle Pool Formation show predominant NW strikes in all sectors (Figure 5b), though this may vary between WNW and NNW. Dikes with NE trends are rare. Banakite (biotite andesite) dikes contemporaneous with the infill of the inner caldera by the Morrisons Pool Formation show predominant NW trends, with variation between E-W and NNW (Figure 5c). A slight preference for NE trends occurs in the N sector. Mapping and drilling indicates that occasional shoshonite and banakite dikes occur adjacent and subparallel to the caldera and may be considered as ring dikes.

4.2. Faults

[14] Faults in the caldera are brittle, 5 cm to 2 m wide zones consisting of varying proportions of gouge, microbreccia, breccia ± foliated cataclasite. They are best exposed over a vertical interval of ~720 m within the Emperor gold mine. Foliated cataclasites are observed at most levels of the mine except within the upper 150 m. They have a crudely to well-manifested ''foliation,'' with the angle between the foliation and the overall zone describing a sense of fault movement in a similar way to S-C geometries in mylonitic rocks [e.g., *Berthe et al.*, 1979; *Simpson and Schmid*, 1983]. This observation is supported by other mesoscopic sense of movement indicators such as offsets markers, tension

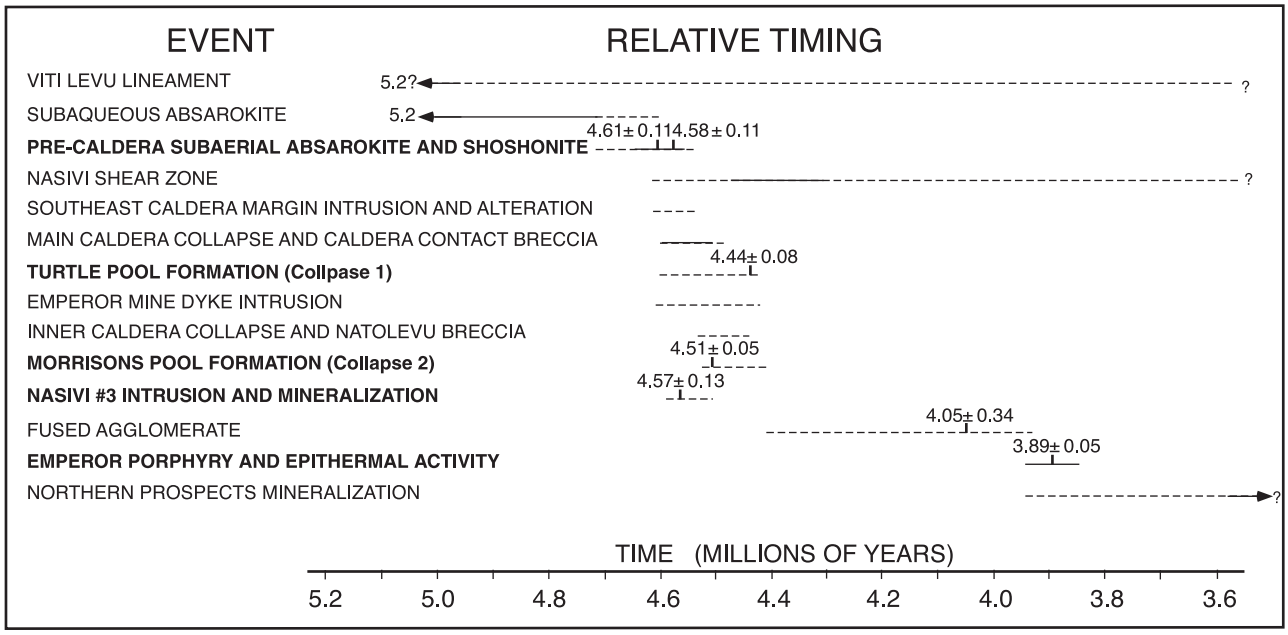

Figure 4. Relative timing of structural, magmatic, and hydrothermal events affecting the Tavua Volcano. Adapted from *Eaton and Setterfield* [1993]. Events are listed in order of relative age deduced from field observations. Solid lines represent well-constrained event; dashed lines represent moderate to poorly constrained event. The ^{40}Ar-^{39}Ar age quoted for the Emperor porphyry and epithermal activity is the weighted mean age of six samples [*Begg*, 1996]. Other quoted ages are from *Setterfield et al.* [1992] and *Begg* [1996].

gashes/veins, quartz-fiber steps and pluck marks [*Tjia*, 1968, 1971] on slickensided surfaces. The foliation is usually either defined by gouge and microbreccia layers of different composition and/or grain size, or by quartz-carbonate vein material alternating with gouge and microbreccia. Faults from deeper parts of the mine often also contain chlorite-rich bands parallel to the foliation. Several episodes of cataclasis ± cementation (generally by silicification) are apparent on many faults. When exposed, faults frequently display at least one well- slickensided surface, preserving the last movement vector. Crosscutting relationships indicate that this last movement episode generally postdates epithermal mineralization.

[15] The most prominent regional fault sets are steeply dipping with WNW, NW, NNE, and E-W strikes (Figure 5d). The ring fault pattern is dominantly composed of a number of throughgoing regional faults, or fault sets, each of which occupies a portion of the overall polygonally shaped caldera margin. The most pronounced ring fault development coincides with the mapped position of the caldera contact. Some faults impinging on the caldera margin at a high angle to the ring faults are terminated at the margin. These are a combination of regional throughgoing faults that must predate infill of the Tavua Caldera, and local radial faults associated with various stages of caldera collapse. A number of faults are manifested within the caldera, and some of these are regional throughgoing faults. The most prominent of these is the WNW trending Nasivi Shear Zone (NSZ), which was active prior to and during the collapse and infill of the Tavua Caldera [*Begg*, 1996]. The NSZ is manifested within the caldera by a series of en echelon faults (Figure 3). Two splits of the NSZ, the Homeward Bound Shear and Shatter Shear, pass through the precaldera stratigraphy in the northern portion of the Emperor gold mine (HBS and SS; Figure 3). The Emperor gold mine is located at a pronounced intersection of regional throughgoing faults and ring faults of the caldera margin, and represents a zone of intense faulting and fracturing.

[16] Fault geometries in the Emperor gold mine form four groups (Figures 5d and 6): (1) north and NNE striking vertical to steeply east dipping ring faults; (2) NW striking steeply SW dipping faults; (3) WNW striking steeply north dipping faults such as the Homeward Bound Shear and Shatter Shear; and (4) thrust faults (also called flatmakes in usage by the Emperor gold mine) with SE, south, or north dips <45° (typically, 20°–35°), 100 m to kilometer length scales and 0.1–3.0 m widths (Figure 6b). The largest thrust fault, the Prince Flatmake, has strike and dip lengths of 1575 m and >1500 m, respectively.

5. Kinematic Analysis of Faults in the Tavua Volcano

[17] Slickenside measurements have been taken from faults and fault zones across the Tavua Volcano, with most data (>95%) from the Emperor gold mine. Where slicken-

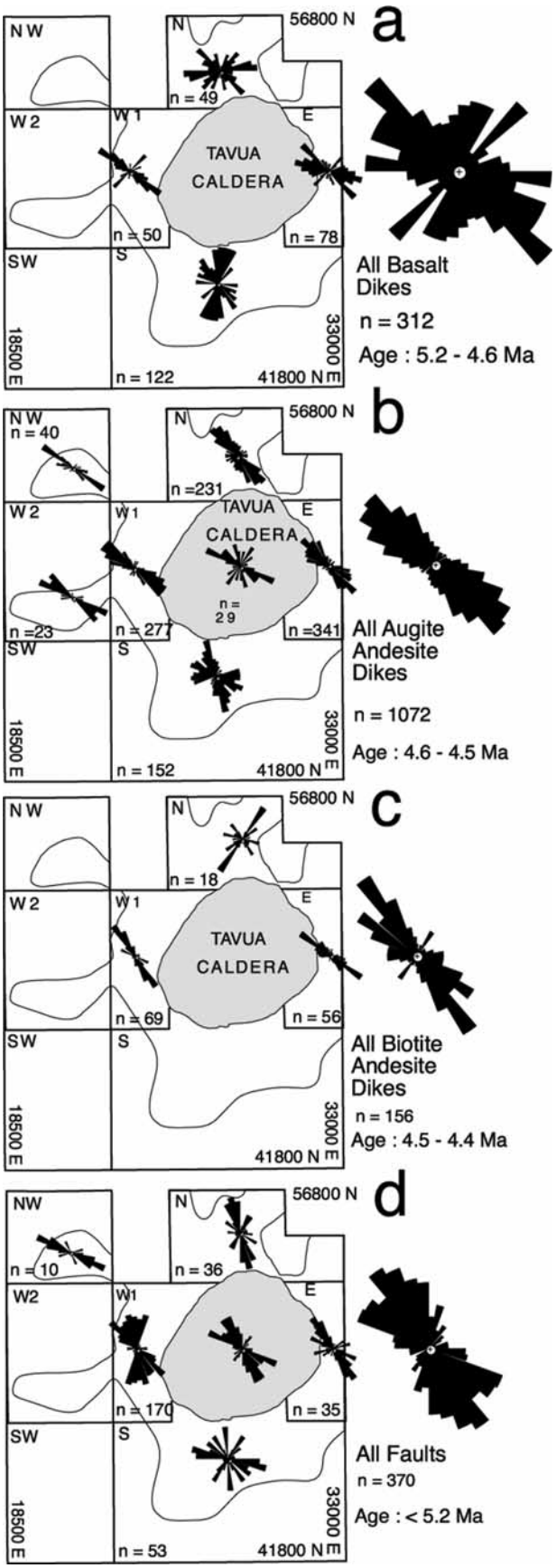

sides are observed in the vicinity of lode structures, they generally postdate the mineralization and preserve evidence of the last slip event to occur. Total slickenside data from the Tavua Volcano (Figure 7a) describes dominant shallow to moderate plunges broadly scattered 50° either side of NNW-SSE. Kamb contouring reveals a strong, shallow plunging maxima trending south, and weaker maxima trending NNW-SSE and WNW (Figure 7b).

[18] Slip normal analysis was undertaken using FaultKin (unpublished computer program, version 3.25a, developed by R. W. Allmendinger, R. A. Marrett, and T. Cladouhos) on the subset of this data (n = 157) that contained fault plane orientation, slickenside lineation, and sense of movement information. Movement senses were obtained from observed offsets, tensional fracture orientations, quartz-fiber steps [*Marshak and Mitra*, 1988], pluck and drag textures [*Petit*, 1987; *Angelier*, 1994, Figure 4.17], and foliation trajectories in foliated gouge and cataclasite. FaultKin was used to calculate the principal incremental shortening axes (*P*), and principal incremental extension axes (*T*), and linked Bingham axes. Each pair of *P* and *T* axes lies in the movement plane containing the slip vector and the normal vector to the fault plane. The axes are at 45° to the vectors. Knowledge of slip direction is required to distinguish between the axes. The linked Bingham axes correspond to the directional maxima of the shortening and extension axes for a given population of faults [*Mardia*, 1972]. They are the equivalent of an unweighted moment tensor summation, where all faults are given equal weight, and the kinematics are assumed to be scale-invariant [*Marrett and Allmendinger*, 1990]. *Marrett and Allmendinger* [1990] point out that this will affect the accuracy of the method, as will any reorientation of the data, sampling bias with respect to the whole fault population, or any spatial heterogeneity of the strain. In this study, any reorientation of the data will be minor, as there is no evidence of significant overprinting deformation. Sampling bias has been ignored.

Figure 5. (opposite) Fault and dike strike orientation data for the Tavua Volcano. The mapped portion of the volcano excludes much of the eastern flank. Most information is derived from the periphery of the Tavua Caldera. The thin solid line encompasses >97% of data, which has been arbitrarily divided into eight sectors to highlight spatial changes in structure orientations about the caldera. (a) Basalt (absarokite) dikes. (b) Augite andesite (shoshonite) dikes. (c) Biotite andesite (banakite) dikes. (d) Faults. Data from the W1 sector are mostly the authors' own, while data in other sectors are mostly derived from WMC mapping. No account is made for dikes of different lengths. Coordinates refer to the local WMC exploration grid, parallel to geographic north. Roses are divided into 10° increments, and petals are not weighted by area, tending to accentuate dominant trends. The "n" value is the number of structures per rose diagram. Approximate ages are given for each group of structures based on field relationships and radiometric age dates from *Whelan et al.* [1985] and *Setterfield et al.* [1992].

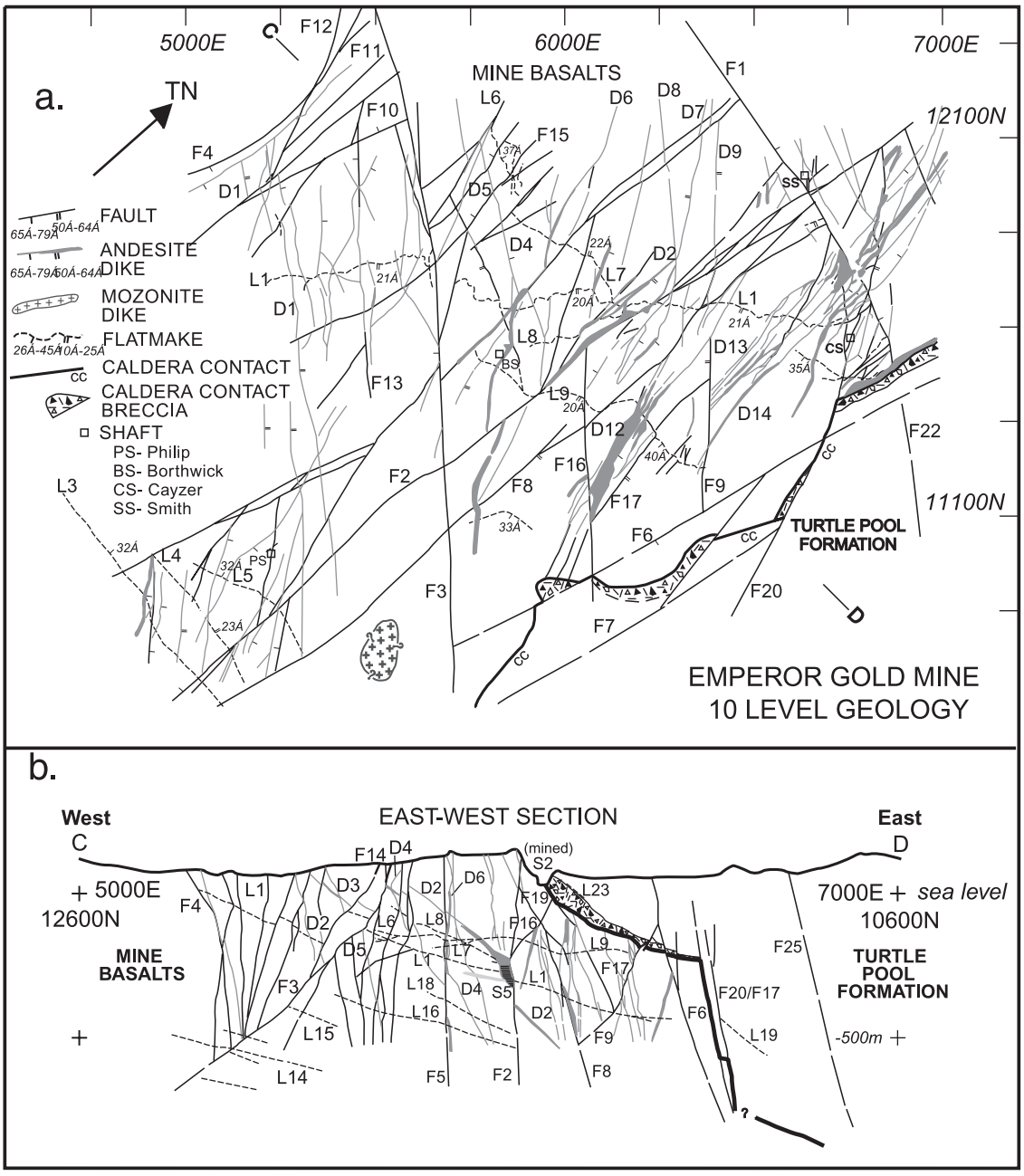

Figure 6. Fault populations within the Emperor gold mine. (a) Map of fault intersections at the 10 level (240 m below sea level) Emperor gold mine constructed from underground mapping. (b) East-west structural profile through the Emperor gold mine showing the caldera contact (delineated by breccia), steep, anastomosing brittle faults, and the gently dipping thrust faults. Individual features are designated by a numbering system for faults (e.g., F1, F2), thrust faults (e.g., L1, L2), and dikes (D1, D2, etc.). Some fault and dike names can be cross-referenced using this numbering system on Figure 10.

Homogeneity of the strain in the mine was tested by examining the linked Bingham axes for data from different tilt blocks in the Emperor gold mine [*Begg*, 1996]. Moderate to good correlation exists between the dominant strain axes clusters in each block. Weighting of the data was qualitatively assessed by comparing the kinematics of the largest faults in the mine, which form reactivated block boundaries (faults F1, F2, F3; Figure 6), with all the (generally smaller displacement) faults from within the blocks. A good correlation exists, thus the fault kinematics are scale-invariant.

[19] The strain axis patterns for all slickenside data are shown in Figures 7c–7f. While the *P* axis data show a strong clustering (Figures 7c and 7d), the *T* axes describe a

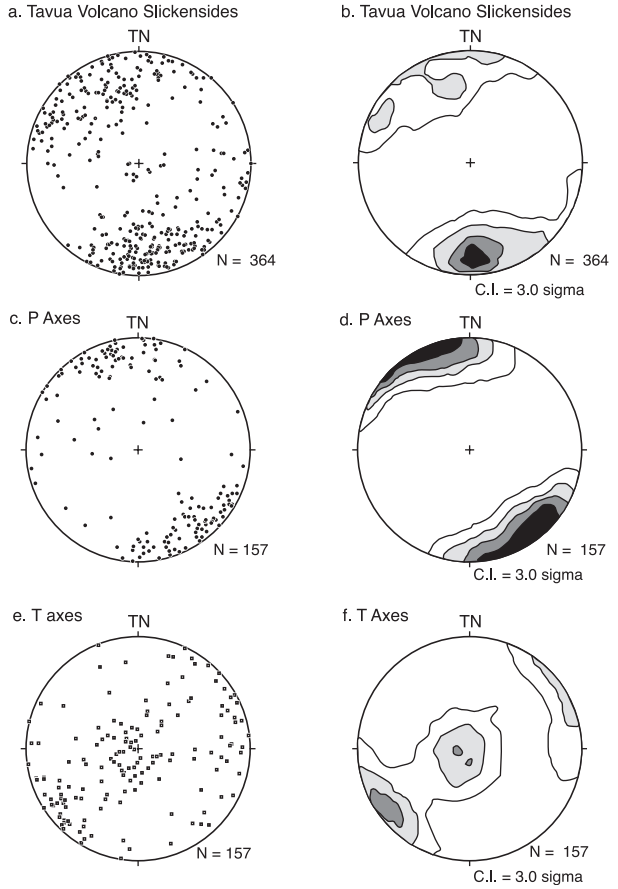

Figure 7. Slipline kinematic summary for all data from the Emperor gold mine, Tavua Volcano. All plots are on equal-area stereonets. Contour plots use intervals of 3σ. Axes are labeled as follows: *P*, principal incremental shortening axes; *T*, principal incremental extension axes. (a) Total slickensides. (b) Contoured slickenside data. (c) *P* axes. (d) Contoured *P* axes. (e) *T* axes. (f) Contoured *T* axes.

girdle pattern (Figures 7e and 7f), indicating kinematically heterogeneous faulting. According to *Marrett and Allmendinger* [1990], this can be attributed to any of four mechanisms: triaxial deformation, anistropy reactivation, strain compatibility constraints, or multiple deformations. Since the first two of these are particularly relevant to the data set, because of the multiplicity of fault orientations, orthorhombic fault patterns [*Begg*, 1996], and reactivated early dike margins and faults, the data have been separated into steep (fault) structures (Figure 8) and gently dipping thrust fault related structures (Figure 9). The latter formed during, or just prior to, the recorded slip events, whereas the faults are reactivated older structures inherited from caldera collapse. The fault kinematics indicate subhorizontal shortening from an average 330°/150° (Figures 8a and 8c), with perpendicular subhorizontal extension (Figures 8b and 8d), while the thrust fault kinematics indicate subhorizontal shortening from an average 342°/162° (Figures 9a and 9c) with perpendicular subvertical extension (Figures 9b and 9d). Both data sets show evidence of a second, smaller cluster of *P* axes, consistent with a component of NE-ENE shortening, and NNW extension.

6. Dikes and Faults as Stress Indicators

[20] Dike trends may be used as stress indicators [e.g., *Ode*, 1957; *Nakamura et al.*, 1977, 1980; *Muller and Pollard*, 1977; *Zoback et al.*, 1981; *Eaton*, 1982, 1984; *Laughlin et al.*, 1983]. *Anderson* [1936, 1951] postulated that volcanic dikes intrude parallel to the local $\sigma_1-\sigma_2$ plane, with either stress vertical, and with σ_3 horizontal, provided the magma pressure exceeded $\sigma_3 + T$, where T is the tensile strength of the rock. Similarly, with sills the $\sigma_1-\sigma_2$ plane would be horizontal and σ_3 therefore vertical. This is in keeping with the Griffith crack theory [e.g., *Jaeger*, 1969; *Roberts*, 1970; *Suppe*, 1985], where a fluid-filled crack will tend to propagate perpendicular to σ_3, similar to a tensile fracture. Planar discontinuities such as bedding, faults,

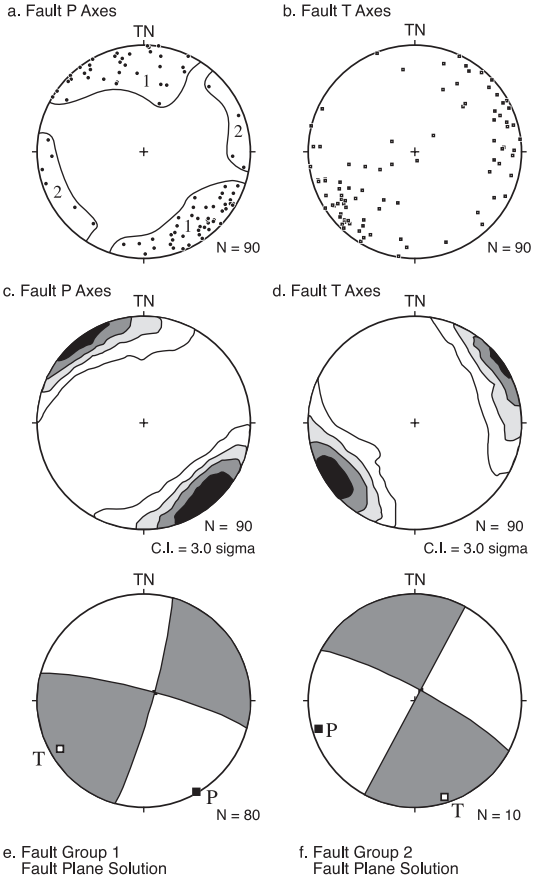

Figure 8. Slipline kinematic summary for faults in the Emperor gold mine, Tavua Volcano. All plots are on equal area stereonets. Contour plots use intervals of 3σ. Principal incremental shortening axes (*P*), principal incremental extension axes (*T*), and linked Bingham axes. (a) *P* axes. (b) *T* axes. (c) Contoured *P* axes. (d) Contoured *T* axes. (e) Fault plane solution including linked Bingham axes for cluster 1 axes. (f) Fault plane solution including linked *Bingham* axes for cluster 2 axes.

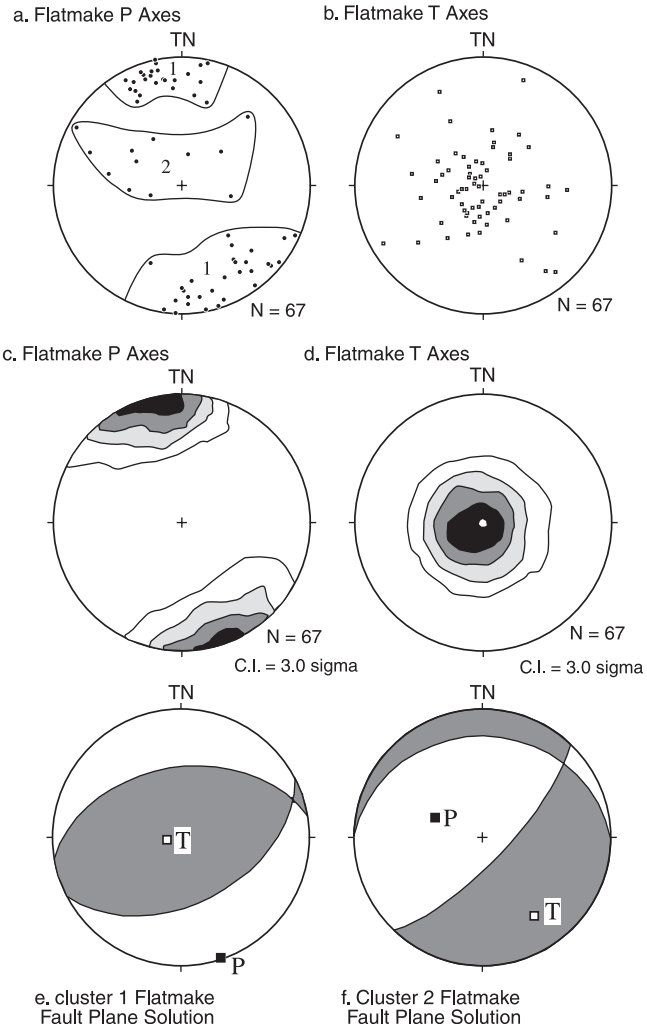

Figure 9. Slipline kinematic summary for thrust faults in the Emperor gold mine, Tavua Volcano. All plots are on equal-area stereonets. Contour plots use intervals of 3σ. Principal incremental shortening axes (*P*), principal incremental extension axes (*T*), and linked Bingham axes are calculated from thrust fault, flatcrack, and short-length (<1 m) fracture data. (a) *P* axes. (b) *T* axes. (c) Contoured *P* axes. (d) Contoured *T* axes. (e) Fault plane solution including linked Bingham axes for cluster 1 axes. (f) Fault plane solution including linked Bingham axes for cluster 2 axes.

joints, and other dikes may cause deviations of dike orientations with respect to the regional stresses [*Pollard*, 1973; *Suppe*, 1985]. Studies of earthquake swarms in active volcanic regions have been used to infer the orientation of dikes [e.g., *Hill*, 1977]. In this study, the average orientation of the principal stresses is assumed to be either horizontal or vertical. When it is uncertain whether σ_1 is horizontal or vertical, as is the case with vertical dikes, it is instructive to refer to the principal stresses as the greatest (σ_H) and least (σ_h) horizontal principal stresses, and the vertical principal stress (σ_v).

[21] Faults can also be used as dynamic indicators, particularly using stress inversion techniques [e.g., *Etchecopar et al.*, 1981; *Angelier*, 1984, 1994; *Gephart and Forsyth*, 1984; *Michael*, 1984; *Reches*, 1987]. Stress inversion assumes that the shortening and extension axes indicated by the slip normal analysis of large slickenline data sets from variably oriented faults can be directly equated with the maximum and minimum compressive stresses, respectively. Coincidence of stress and strain axes requires that (1) the regional stress tensor must be spatially and temporally homogeneous and (2) that fault surface slip must have the same direction and sense as the maximum shear stress resolved on each surface from the regional stress field [see *Pollard et al.*, 1993].

6.1. Dikes

[22] On Viti Levu in the vicinity of the Tavua Volcano, absarokite, shoshonite, and banakite dikes have dominant NW trends (Figures 5a–5c), indicative of a NW σ_H. These trends persist across the volcano and within the Tavua Caldera. There is some variability of the data, particularly for the absarokite dikes (Figure 5a), possibly indicating that a NNE-NE σ_H may have preceded and, in part, overlapped with a WNW-NW σ_H. Regional mapping by the Fiji Mineral Resources Department reveals that dikes of probable Pliocene age throughout the Fiji Islands are dominated by broadly NW to north trends [e.g., *Bartholomew*, 1960; *Coulson*, 1971; *Woodrow*, 1976]. A second, weaker population of NE to east striking dikes has also been observed.

[23] Detailed study of dikes in the Emperor gold mine reveals that dike trajectories deviate from the regional average trend in the vicinity of the caldera contact (Figure 3). This only occurs within a radius of ~1 km from the major caldera contact fault zone on the eastern margin of the mine, and modeling of the stress field [*Begg*, 1996] suggests that this is related to modification of the regional stress field by the stresses associated with caldera collapse. Dike orientations are therefore considered representative of the resultant stress field. Precaldera absarokite (basalt) dike trends (Figure 5a) show an almost radial geometric distribution, possibly because of relatively large magma pressures compared with the regional deviatoric stresses [cf. *Suppe*, 1985]. Alternatively, these trends can be resolved into two groups, representing a WNW-NW compression direction and a weaker NNE-NE compression direction. The syncaldera shoshonite and banakite dikes (Figures 5b and 5c) indicate a strong NW σ_H.

6.2. Faults

[24] Steep fault and thrust fault movement senses have been used to constrain the principal horizontal compression direction (σ_1) operative after infill of the caldera (Figure 10). The fault data can be broken into prethrust fault, synthrust fault, and postthrust fault movements, but as both synthrust fault and postthrust fault offsets indicate a similar domain of compression, they are summarized on the one diagram (Figure 10b). To satisfy the strike-slip components of movement, the faults must have moved in response to horizontal compression between 332° and 002° (Figure 10b), while the

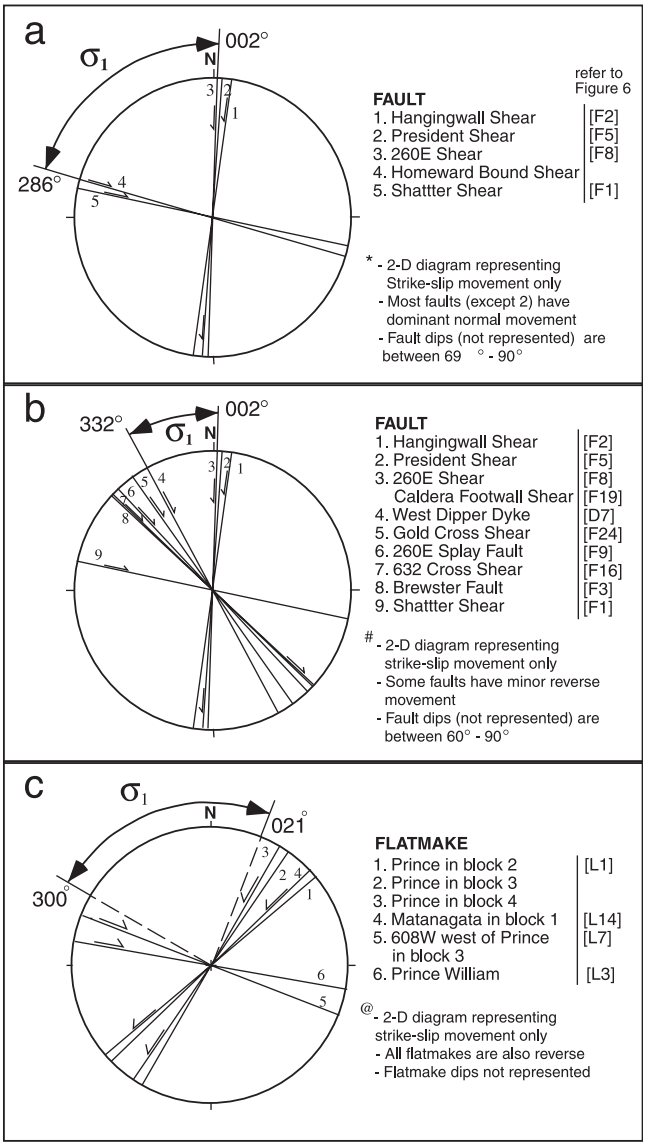

Figure 10. Inferred stress diagrams for Emperor gold mine faults and thrust faults. (a) Prethrust fault kinematics (see asterisk). (b) Synthrust fault/postthrust fault kinematics (see number symbol). (c) Thrust fault kinematics (see the "at" symbol). Movement sense is indicated by the half arrow on particular fault structures. Note the principal horizontal stress direction (σ_1) occupies the region of inward directed movement, delineated by the bold circular arrow. The numbers in square brackets refer to the fault and dike numbering system in Figure 6. The σ_1 domain for thrust faults is constrained by the normals to the Prince Flatmake in block 4, and the 608W hanging wall thrust fault.

thrust faults must have formed under horizontal compression between 300° and 021° (Figure 10c). Thus the domain of compression for the faults is compatible with synchronous thrust fault development. The broad range of possible shortening directions indicated for the thrust faults reflects the large strike difference between those with sinistral movement sense and those with dextral movement sense. A shortening direction of 336° for thrust fault formation has been derived from their orthorhombic symmetry (Figure 10c).

[25] The 12° difference between the slipline analysis shortening direction indicated for the steep faults versus that indicated for the thrust faults indicates that at least one of fault groups is slightly noncoaxial with respect to the regional stress. As the steep faults are older (i.e., predate caldera collapse) these structures have been reactivated during caldera collapse and thrust fault development, and they are therefore more likely to be slightly noncoaxial with respect to the regional stress field. By examination of offset markers, prethrust fault strike-slip movement has been documented for a number of faults, and it corresponds with the strike-slip component of oblique-slip occurring during caldera collapse. To satisfy this strike-slip component of movement, the principal horizontal compression direction must have been between 286° and 002° (Figure 10a). This interval contains that indicated for the dikes.

7. Stress Geometries With Time and the Tavua Volcano

[26] The occurrence of steep dikes throughout the volcanic history testifies to a vertical farfield $\sigma_1-\sigma_2$ plane, with horizontal σ_3. A horizontal σ_1 is consistent with both the prethrust fault and postthrust fault oblique-slip component of movement on steep faults. During caldera collapse, movement on these faults would have been mostly normal, particularly during periods of rapid collapse, when σ_1 would have been (at least locally) vertical. Formation of the thrust faults, which occurred subsequent to infill of the Tavua Caldera, resulted from a horizontal $\sigma_1-\sigma_2$ plane, vertical extension (σ_3), and with σ_1 approximately NNW (Figure 10c). Kinematic analysis of thrust fault slickensides, which generally overprint the mineralization associated with thrust fault formation, indicates the same stress geometry (Figure 8). The en echelon nature of steep faults forming the Nasivi Shear Zone in the center of the caldera (Figure 3) is consistent with a broadly NW-NNW shortening and a horizontal σ_1. These faults formed immediately following eruption of the banakite lavas in the Inner Caldera.

[27] The onset of the horizontal shortening (response to horizontal σ_1) from the NW quarter is constrained to sometime during building of the upper, subaerial portion of the volcano (period of absarokite dike intrusion) shortly before caldera collapse at 4.6 Ma. Apart from some local fluctuations during periods of rapid collapse, σ_1 remained horizontal until at least after thrust fault formation at 3.9 Ma [*Setterfield et al.*, 1992; *Begg*, 1996]. During this time, flipping of the σ_2 and σ_3 axes can be invoked to explain the variation from steep structures formed under a horizontal σ_3, such as dikes and normal faults, to gently dipping sills and thrust faults formed under a vertical σ_3.

8. Implications for the Tectonic Development of Fiji

[28] Dike orientations and fault movement histories have been used as the basis for stress analysis of successive

Table 1. Stress History of the Tavua Volcano Showing the Compression Direction Through Time for Particular Stress Indicators[a]

Data Source	Compression Direction	Age, Ma
Absarokite dikes	WNW-NW (281°–340°)	5.2–4.6
	NNE-NE (010°–050°)	5.2–4.6
Shoshonite dikes	NW (305°–314°)	4.6–4.5
Banakite dikes	NW (299°–327°)	4.5–4.4
Prethrust faulting	WNW-N (286°–002°)	4.5–4.4
Thrust fault fractures	NW-NNE (300°–021°)	3.9
Thrust fault group geometries	NNW (336°)	3.9
Synthrust/postthrust faulting	NNW-N (332°–002°)	≤3.9
Late fault slickenlines	NW-NNW (307°–341°)	<3.9
Late thrust fault slickenlines	NNW-N (328°–360°)	<3.9
Recent seismicity	north (Fiji Platform)	0
	NE (north of Fiji)	0

[a] Absolute ages take into account field relationships as well as ^{40}Ar-^{39}Ar dating results from *Setterfield et al.* [1992] and from *Begg* [1996]. Seismicity data (focal mechanism solutions) are from *Hamburger and Isacks* [1988].

structural and magmatic events (Table 1 and Figure 11). These data suggest that the NW σ_1 has rotated ~50° (minimum 45°, maximum 60°) in a clockwise direction (from WNW to NNW) since the period ~5.0–4.6 Ma, the time of intrusion of the WNW-NW trending absarokite dikes (Figure 11). Alternatively, these data may be construed as indicating a more or less constant N-S σ_1, and 50° counterclockwise rotation of the Fiji Platform. This latter hypothesis is consistent with previous suggestions by many other workers [e.g., *Falvey*, 1978; *Malahoff et al.*, 1982; *Whelan et al.*, 1985] that substantial counterclockwise rotation of the Fiji Platform has occurred since fragmentation of the formerly continuous Outer Melanesian Arc during the latest Miocene to earliest Pliocene (Figures 1c–1e). Paleomagnetic studies [*Malahoff et al.*, 1982; *Whelan et al.*, 1985, *Taylor et al.*, 2000] and geological reconstructions based on land geology [*Green and Cullen*, 1973], and geochemistry [*Gill and Gorton*, 1973], have previously been used to infer up to 90° counterclockwise rotation of the Fiji Platform since the Miocene, with best estimates considered to be 21°–60° [*Whelan et al.*, 1985]. Paleomagnetic work by *Taylor et al.* [2000] indicates up to 135° rotation between 10 Ma and 3 Ma. The latter is compatible with the current ENE-WSW trend of the exposed axis of the lower Oligocene to middle Miocene Wainimala arc (Figure 2). This study provides important constraints not only on the amount of progressive rotation, but also on the rate and timing of the rotation. A 50° rotation since ~5 Ma indicates an average of ~10° Myr^{-1}. This incorporates a period of particularly fast rotation of ~24° Myr^{-1} from ~5.0 Ma to 3.9 Ma. *Taylor et al.* [2000], however, postulate that rotation of the Fiji platform stopped abruptly at 3 Ma with the development of a well-defined spreading center in the North Fiji Basin. This infers that the entire 50° rotation occurred between ~5 Ma and 3 Ma, at a rate of ~25° Myr^{-1}. Knowledge of the rotation history allows for calculation of the original orientation of geological features, depending on their age of formation. For instance, the ENE trending Viti Levu lineament, with an age of at least 5.2 Ma, would originally have had a ESE to SE trend, assuming that the Fiji Platform rotated as a coherent mass. Many of the largest faults on Viti Levu and Vanua Levu have NE-ENE (formerly E-ESE) strikes. Significant lateral slip on these structures within the Fiji Platform may have "absorbed" some of the rotation. However, this is considered unlikely,

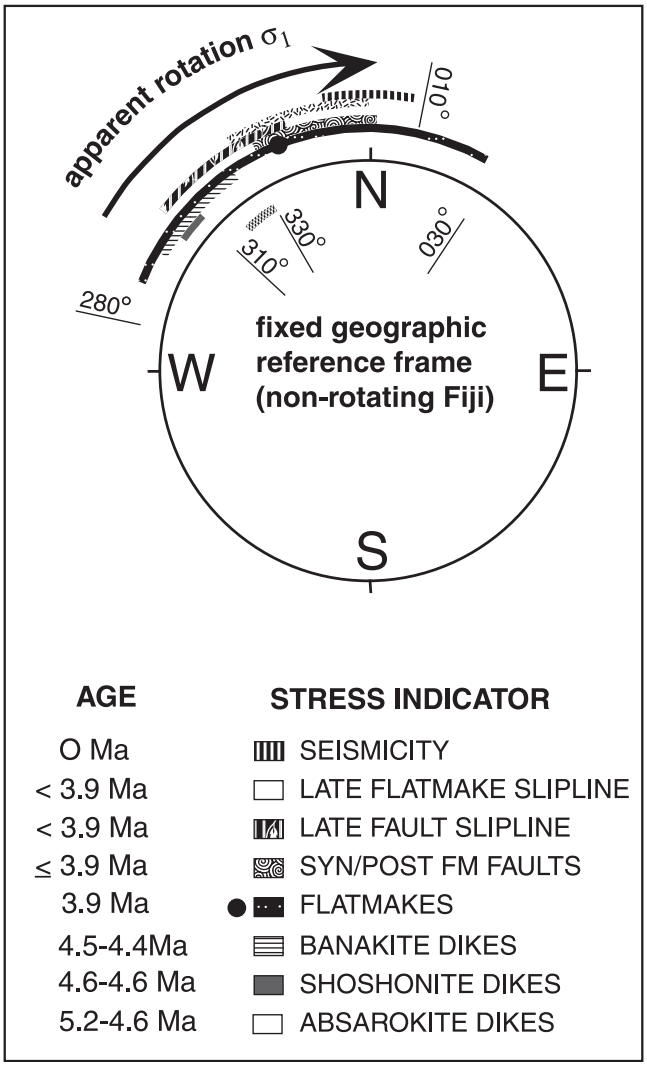

Figure 11. Stress history summary diagram for the Tavua Volcano. Domains of compression axes for all stress indicators are arranged in chronological order from oldest (innermost) to youngest (outermost) and plotted with respect to present-day geographic coordinates. These data are compared with shortening directions (±10°) indicated in recent studies of seismicity about the Fiji Platform by *Hamburger and Isacks* [1988], and typical paleomagnetic declinations (320°–330°) for 4–5 Ma rocks (inside circle of geographic reference). Assuming a fixed geographic reference frame, there is an apparent progressive change in stress orientation with time. The outer bold arrow indicates an apparent 45°–90° clockwise rotation of σ_1 with time. "FM" is abbreviation for flatmake.

as throughout much of the rotation history such faults would have been unfavorably oriented for slip, having a >50° strike disparity with a N-S σ_1 [cf. *Sibson*, 1990].

[29] The late Miocene to Pliocene geological features of the Fiji Platform, counterclockwise rotation, and the onset of N-S compression sometime between ~5.0 Ma and 4.6 Ma, can be understood in relation to the events precipitated by the late Miocene collision between the east facing arc and the oceanic plateaus of the Melanesian Borderlands (Figures 1d and 1e). Collision is likely responsible for termination of Wainimala arc volcanism and late Miocene uplift, folding, and faulting [*Hathway*, 1993; *Rodda*, 1993]. Subduction flipping and initiation of the Vanuatu trench is likely to have encouraged NE-SE extension and the formation of SE-NW trending sedimentary basins (e.g., Nadi, Sovi, and Navua Basins on Viti Levu; now trending ENE-WSW in Figure 2) and volcanic ''lineaments'' (e.g., Viti Levu Lineament; Figure 2). An E-W transfer zone, incorporating the Fiji Platform, connected the opposite facing Tonga and Vanuatu subduction zones, which began to diverge as a consequence of subduction hinge migration. Counterclockwise rotation of the Fiji Platform occurred because of the combined effect of the opening of the North Fiji Basin behind the Vanuatu arc, and the left lateral slip on the E-W transfer zone incorporating the platform (Figure 1d). The need to accommodate northward translation of the Australian Plate resulted in N-S compression across the growing transfer zone. Shortly before 4.6 Ma, this compression began to be felt with greater intensity as rotation of the platform caused misorientation of major faults and volcanic lineaments with respect to the compression. This resulted in early Pliocene basin inversion [*Hathway*, 1993; *Rodda*, 1993], the decline of volcanic activity along the Viti Levu lineament, and a period of particularly rapid (~25° Myr^{-1}) rotation of the platform. Subduction was initiated along the Hunter Fracture Zone [*Rodda*, 1993].

[30] **Acknowledgments.** The paper is part of Ph.D. research undertaken by G. Begg at Monash University while on study leave from Western Mining Corporation Limited (WMC). The work was supported by an Australian Postgraduate Research Industry Award (APRAI) and a grant from WMC and Emperor Gold Mining Company Limited (EGM). G. Begg thanks Peter Eaton for stimulating discussions and Mohammed Azam and Gabe Faga for support and geological assistance in the mine.

References

Anderson, E. M., The dynamics of the formation of cone sheets, ring dikes, and cauldron subsidences, *R. Soc. Edinburgh Proc.*, *56*, 128–157, 1936.

Anderson, E. M., *The Dynamics of Faulting*, 206 pp., Oliver and Boyd, White Plains, N. Y., 1951.

Anderson, W. B., and P. C. Eaton, Gold mineralization at the Emperor mine, Vatukoula, Fiji, *J. Geochem. Explor.*, *36*, 267–296, 1990.

Angelier, J., Tectonic analysis of fault slip data sets, *J. Geophys. Res*, *89*, 5835–5848, 1984.

Angelier, J., Fault slip analysis and paleostress reconstruction, in *Continental Deformation*, edited by P. L. Hancock, pp. 53–100, Pergamon, New York, 1994.

Arthaud, F., Méthode de détermination graphique des directions de raccourcissement, d'allongement et intermédiare d'une population de failles, *Bull. Soc. Geol. Fr.*, *7*, 729–737, 1969.

Bartholomew, R. W., Geology of the Nandi Area, *Fiji Miner. Resour. Div. Bull.*, *7*, 68 pp., 1960.

Begg, G. C., *Genesis of the Emperor Gold Deposit, Fiji*, Ph.D. thesis, Monash Univ., Melbourne, Australia, 1996.

Berthe, D., P. Choukroune, and P. Jegouzo, Orthogenesis, mylonite and non-coaxial deformation of granites: The example of the south Armorican shear zone, *J. Struct. Geol.*, *1*, 31–42, 1979.

Chase, C. G., Tectonic history of the Fiji Plateau, *Geol. Soc. Am. Bull.*, *82*, 3087–3110, 1971.

Colley, H., and W. H. Hindle, Volcano-tectonic evolution of the Fiji and adjoining marginal basins, in *Marginal Basin Geology: Volcanic and Associated Sedimentary and Tectonic Processes in Modern and Ancient Marginal Basins*, edited by B. P. Kokelaar and M. F. Howells, *Geol. Soc. Spec. Publ.*, *16*, 151–162, 1984.

Coulson, F. I. E., Geology of western Vanua Levu, *Fiji Miner. Resour. Div. Bull.17*, 86 pp., 1971.

Eaton, G. P., The Basin and Range province: Origin and tectonic significance, *Annu. Rev. Earth Planet. Sci.*, *10*, 409–440, 1982.

Eaton, G. P., The Miocene Great Basin of western North America as an example of an extending back-arc region, *Tectonophysics*, *102*, 275–295, 1984.

Eaton, P. C., and T. N. Setterfield, The relationship between epithermal and porphyry systems within the Tavua Caldera, Fiji, *Econ. Geol.*, *88*, 1053–1083, 1993.

Etchecopar, A., G. Vasseur, and M. Daignieres, An inverse problem in microtectonics for the determination of stress tensors from fault striation analysis, *J. Struct. Geol.*, *3*, 51–65, 1981.

Falvey, D. A., Arc reversals, and a tectonic model for the North Fiji Basin, *Aust. Soc. Explor. Geophys. Bull.*, *6*, 47–49, 1975.

Falvey, D. A., Analysis of palaeomagnetic data from the New Hebrides, *Aust. Soc. Explor. Geophys. Bull.*, *9*, 117–123, 1978.

Gephart, J. W., and D. W. Forsyth, An improved method for determining the regional stress tensor using earthquake focal mechanism data: Application to the San Fernando earthquake sequence, *J. Geophys. Res.*, *89*, 9305–9320, 1984.

Gill, J. B., and M. P. Gorton, A proposed geological and geochemical history of eastern Melanesia, in *The Western Pacific: Island Arcs, Marginal Seas, Geochemistry*, edited by P. J. Coleman, pp. 459–467, Univ. of West. Aust. Press, Perth, 1973.

Gill, J. B., and I. McDougall, Biostratigraphic and geological significance of Miocene-Pliocene volcanism in Fiji, *Nature*, *241*, 176–180, 1973.

Gill, J. B., and P. Whelan, Early rifting of an oceanic island arc (Fiji) produced shoshonitic to tholeiitic basalts, *J. Geophys. Res.*, *94*, 4561–4578, 1989.

Gill, J. B., A. L. Stork, and P. Whelan, Volcanism accompanying back-arc basin development in the southwest Pacific, *Tectonophysics*, *102*, 207–224, 1984.

Goscombe, B. D., and J. L. Everard, Tectonic evolution of Macquarie Island: Extensional structures and block rotations in oceanic crust, *J. Struct. Geol.*, *23*, 639–673, 2001.

Green, D., and D. J. Cullen, The Tectonic Evolution of the Fiji Region, in *The Western Pacific: Island Arcs, Marginal Seas, Geochemistry*, edited by P. J. Coleman, pp. 127–145, Univ. of West. Aust. Press, Perth, 1973.

Hamburger, M. W., and I. B. Everingham, Seismic and aseismic zones in the Fiji region, *Bull. R. Soc N. Z.*, *24*, 439–453, 1986.

Hamburger, M. W., and B. L. Isacks, Diffuse back-arc deformation in the southwestern Pacific, *Nature*, *332*, 599–604, 1988.

Hamburger, M. W., I. B. Everingham, B. L. Isacks, and M. Barazangi, Active tectonism within the Fiji platform, southwest Pacific, *Geology*, *16*, 237–241, 1988.

Hathway, B., The Nadi Basin: Neogene strike-slip faulting and sedimentation in a fragmented arc, Western Viti Levu, Fiji, *J. Geol. Soc. London*, *150*, 563–581, 1993.

Hathway, B., Sedimentation and volcanism in an Oligocene-Miocene arc and fore-arc, southwestern Viti Levu, Fiji, *J. Geol. Soc. London*, *151*, 499–514, 1994.

Hill, D., A model for earthquake swarms, *J. Geophys. Res.*, *82*, 1347–1352, 1977.

Jaeger, J. C., *Elasticity, Fracture and Flow with Engineering and Geological Applications*, 268 pp., Chapman and Hall, New York, 1969.

Kroenke, L. W., Cenozoic tectonic development of the southwest Pacific, *UN ESCAP, CCOP/SOPAC Tech. Bull.*, *6*, 111–122, 1984.

Laughlin, A. W., M. J. Aldrich, and D. T. Vaniman, Tectonic implications of mid-Tertiary dikes in west-central New Mexico, *Geology*, *11*, 45–48, 1983.

Malahoff, A., S. R. Hammond, J. J. Naughton, D. L. Keeling, and R. N. Richmond, Geophysical evidence for post-Miocene rotation of the Island of Viti Levu, Fiji, and its relationship to the tectonic development of the North Fiji Basin, *Earth Planet. Sci. Lett.*, *57*, 398–414, 1982.

Mardia, K. V., *Statistics of Directional Data*, Academic, San Diego, Calif., 1972.

Marrett, R., and R. W. Allmendinger, Kinematic analysis of fault-slip data, *J. Struct. Geol.*, *12*, 973–986, 1990.

Marshak, S., and G. Mitra, *Basic Methods of Structural Geology*, 446 pp., Prentice-Hall, Old Tappan, N. J., 1988.

Michael, A. J., Determination of stress from slip data: Faults and folds, *J. Geophys. Res.*, *89*, 11,517–11,526, 1984.

Morrison, G. W., Characteristics and tectonic setting of the shoshonite rock association, *Lithos*, *13*, 97–108, 1980.

Muller, O. H., and D. D. Pollard, The stress state near

Spanish Peaks, Colorado, determined from a dike pattern, *Pure Appl. Geophys.*, *115*, 69–86, 1977.

Musgrave, R. J., and J. V. Firth, Magnitude and timing of New Hebrides arc rotation: Paleomagnetic evidence from Nendo, Solomon Islands, *J. Geophys. Res.*, *104*, 2841–2853, 1999.

Nakamura, K., K. H. Jacob, and J. N. Davies, Volcanoes as possible indicators of tectonic stress orientation, Aleutians and Alaska, *Pure Appl. Geophys.*, *115*, 87–100, 1977.

Nakamura, K., G. Plafker, K. H. Jacob, and J. N. Davies, A tectonic stress trajectory map of Alaska using information from volcanoes and faults, *Bull. Earthquake Res. Inst.*, *55*, 89–100, 1980.

Ode, H., Mechanical analysis of the dike pattern of the Spanish Peaks area, Colorado, *Geol. Soc. Am. Bull.*, *68*, 567, 1957.

Parson, L. M., J. A. Pearce, B. J. Murton, R. A. Hodgkinson, and R. C. D. S. Party, Role of ridge jumps and ridge propagation in the tectonic evolution of the Lau back-arc basin, southwest Pacific, *Geology*, *18*, 470–473, 1990.

Petit, J. P., Criteria for the sense of movement on fault surfaces in brittle rocks, *J. Struct. Geol.*, *9*, 597–608, 1987.

Pollard, D. D., Derivation and evaluation of a mechanical model for sheet intrusion, *Tectonophysics*, *19*, 233–269, 1973.

Pollard, D. D., S. D. Saltzer, and A. M. Rubin, Stress inversion methods: Are they based on faulty assumptions?, *J. Struct. Geol.*, *15*, 1045–1054, 1993.

Reches, Z., Determination of the tectonic stress tensor from slip along faults that obey the Coulomb Yield, *Tectonophysics*, *6*, 849–861, 1987.

Recy, J., and J. Dupont, The south-west Pacific: Structural data, 1:12,000,000 map, *rep. 97*, ORSTOM, Paris, 1982.

Roberts, J. L., The intrusion of magma into brittle rocks, in *Mechanism of Igneous Intrusion*, *Geol. J. Spec. Issue*, vol. 2, edited by N. Newall and H. Rast, pp. 287–338, Liverpool Geol. Soc., UK, 1970.

Rodda, P., Outline of the geology of Viti Levu, *N. Z. J. Geol. Geophys.*, *10*, 1260–1273, 1967.

Rodda, P., Geology of Fiji, in *Contributions to the Marine and On-Land Geology and Resource Assessment of the Tonga-Lau-Fiji Region*, edited by A. J. Stevenson, R. H. Herzer, and P. F. Ballance, *SOPAC Tech. Bull.*, *8*, 120 pp., 1993.

Rodda, P., and L. W. Kroenke, Fiji, a fragmented arc, in *Cenozoic Tectonic Development of the Southwest Pacific*, edited by L. W. Kroenke, *CCOP/SOPAC Tech. Bull.*, *6*, 87–109, 1984.

Setterfield, T. N., P. C. Eaton, W. J. Rose, and R. S. J. Sparks, The Tavua Caldera, Fiji: A complex shoshonitic caldera formed by concurrent faulting and downsagging, *J. Geol. Soc. London*, *148*, 115–127, 1991.

Setterfield, T. N., A. E. Mussett, and R. D. J. Oglethorpe, Magmatism and associated hydrothermal activity during the evolution of the Tavua Caldera: ^{40}Ar-^{39}Ar dating of the volcanic, intrusive, and hydrothermal events, *Econ. Geol.*, *87*, 1130–1140, 1992.

Sibson, R. H., Rupture nucleation on unfavorably oriented faults, *Bull. Seismol. Soc. Am.*, *80*, 1580–1604, 1990.

Simpson, C., and S. M. Schmid, An Evaluation of the criteria to deduce the sense of movement in sheared rocks, *Geol. Soc. Am. Bull.*, *94*, 1281–1288, 1983.

Suppe, J., *Principles of Structural Geology*, Prentice-Hall, Old Tappan, N. J., 1985.

Taylor, G. K., J. Gascoyne, and H. Colley, Rapid rotation of Fiji: Paleomagnetic evidence and tectonic implications, *J. Geophys. Res.*, *105*, 5771–5781, 2000.

Tjia, H. D., Fault-plane markings, paper presented at XXIII International Geological Congress, Prague, Czecholslovakia, 1968.

Tjia, H. D., Fault movement, reoriented stress field and subsidiary structures, *Pac. Geol.*, *5*, 49–70, 1971.

Whelan, P., J. B. Gill, E. Kollman, R. A. Duncan, and R. E. Drake, Radiometric dating of magmatic stages in Fiji, in *Geology and Offshore Resources of Pacific Islands Tonga Region*, *Earth Sci. Ser.*, vol. 2, edited by D. W. Scholl and T. W. Vallier, chap. 32, pp. 414–440, Circum-Pac. Counc. for Energy and Miner. Resour., Houston, Tex., 1985.

Woodrow, P. J., Geology of southeastern Vanua Levu, *Fiji Miner. Resour. Div. Bull.*, *4*, 34 pp., 1976.

Zoback, M. L., R. E. Anderson, and G. A. Thompson, Cainozoic evolution of the state of stress and style of tectonism of the Basin and Range province of the western United States, *Philos. Trans. R. Soc. London, Ser. A*, *300*, 407–434, 1981.

G. Begg, Western Mining Corporation (WMC) Resources, P.O. Box 91, Belmont, WA 6104, Australia. (graham.begg@wmc.com)

D. R. Gray, School of Earth Sciences, The University of Melbourne, Melbourne, VIC 3010, Australia. (drgray@unimelb.edu.au)

View publication stats